Supplementary supporting text

Mouse nomenclature

WT: Wild-type
KO / COL4A3KO: Null for a3 chain of type IV collagen, mouse model for Alport Sydrome
Rag-1 KO: Null for Rag-1, lacks B and T lymphocytes
CD11b KO: Null for CD11b, lacks mature macrophages
COL4A3, Rag-1 DKO / DKO: Null for a3 chain of type IV collagen as well as lacks B and T lymphocytes
C57KO $^{BMT\ C57WT}$ / COL4A3KO $^{BMT\ WT}$: COL4A3KO mouse on C57Bl/6 genetic background transplanted with bone marrow from a WT mouse on C57Bl/6 genetic background.
C57KO $^{BMT\ C57KO}$ / COL4A3KO $^{BMT\ COL4A3KO}$: COL4A3KO mouse on C57Bl/6 genetic background transplanted with bone marrow from a WT mouse on C57Bl/6 genetic background.
129KO $^{BMT\ 129WT}$: COL4A3KO mouse 129Sv genetic background transplanted with bone marrow from a COL4A3KO mouse on 129Sv genetic background.
129KO $^{BMT\ 129KO}$: COL4A3KO mouse 129Sv genetic background transplanted with bone marrow from a COL4A3KO mouse on 129Sv genetic background.
129KO $^{BMT\ C57WT}$: COL4A3KO mouse 129Sv genetic background transplanted with bone marrow from a WT mouse on C57Bl/6 genetic background.
129KO $^{BMT\ C57KO}$: COL4A3KO mouse 129Sv genetic background transplanted with bone marrow from a COL4A3KO mouse on C57Bl/6 genetic background.
KO + WT BM: 20 weeks-old COL4A3KO mouse on C57Bl/6 genetic background infused with bone marrow from a WT mouse on C57Bl/6 genetic background.
KO + KO BM: 20 weeks-old COL4A3KO mouse on C57Bl/6 genetic background infused with bone marrow from a COL4A3KO mouse on C57Bl/6 genetic background.
KO + 8 wk WT transfusion: 8 weeks-old COL4A3KO mouse on C57Bl/6 genetic background transfused with bone marrow from a WT mouse on C57Bl/6 genetic background.
KO + 23 wk WT transfusion: 23 weeks-old COL4A3KO mouse on C57Bl/6 genetic background infused with bone marrow from a WT mouse on C57Bl/6 genetic background.
KO + 23 wk KO transfusion: 23 weeks-old COL4A3KO mouse on C57Bl/6 genetic background infused with bone marrow from a COL4A3KO mouse on C57Bl/6 genetic background.
KO $^{BMi8\ WT}$ 8 weeks-old COL4A3KO mouse on C57Bl/6 genetic background infused with bone marrow from a WT mouse on C57Bl/6 genetic background.
KO $^{BMi8\ KO}$ 8 weeks-old COL4A3KO mouse on C57Bl/6 genetic background infused with bone marrow from a COL4A3KO mouse on C57Bl/6 genetic background.
COL4A3KO $^{BMT\ CD11bKO}$ COL4A3KO mouse on C57Bl/6 genetic background transplanted with bone marrow from a CD11bKO mouse on C57Bl/6 genetic background.

COL4A3KO + Rag-1 KO BMT: COL4A3KO mouse on C57Bl/6 genetic background transplanted with bone marrow from a Rag-1KO mouse on C57Bl/6 genetic background.
KO + Differentiated mESCs: COL4A3KO mouse on C57Bl/6 genetic background injected with differentiated mouse embryonic stem cells derived from a mouse on the C57Bl/6 genetic background.
KO + podocytes: COL4A3KO mouse on C57Bl/6 genetic background injected with immortalized mouse podocyte cell line
KO + mESCs: COL4A3KO mouse on C57Bl/6 genetic background injected with undifferentiated mouse embryonic stem cells derived from a mouse on the C57Bl/6 genetic background.
DKO $^{w/hESCs}$: DKO mouse on C57Bl/6 genetic background injected with undifferentiated human embryonic stem cells (H1 line).
pWT: WT mouse on C57Bl/6 genetic background with COL4A3KO parabiont mouse on the C57Bl/6 genetic background.
pKO: COL4A3KO mouse on C57Bl/6 genetic background with WT parabiont mouse on the C57Bl/6 genetic background.

Wild-type bone marrow-derived cells provides greater histological improvement when compared with COL4A3 KO bone marrow transplanted COL4A3 KO mice

Although total body irradiation may provide some phenotypic improvement in COL4A3 KO mice, an assessment of the specific therapeutic potential of bone marrow-derived cells requires further careful analyses. To assess the therapeutic effect of total body irradiation on the disease progression in bone marrow transplanted COL4A3KO mice, we evaluated renal histology in wild-type (WT), COL4A3 KO (KO), COL4A3 KO transplanted with COL4A3 KO bone marrow, and COL4A3 KO transplanted with WT bone marrow mice. Eight weeks-old C57BL/6 COL4A3 KO mice were transplanted with C57BL/6 bone marrow cells from WT and COL4A3 KO donors and euthanized at 21 weeks of age, 13 weeks post total body irradiation and bone marrow transplantation. The extent of kidney damage, measured by percent normal glomeruli, relative interstitial volume, and tubular atrophy, is significantly reduced in KO transplanted with WT bone

marrow compared to KO and KO mice transplanted with COL4A3 KO bone marrow (**Supplementary Figure 1**). Percent normal glomeruli assessment reveals vast improvement when sub-lethally irradiated COL4A3 KO mice are rescued with WT bone marrow (61.6 ± 6.1%) versus COL4A3 KO bone marrow (29.6 ± 9.0%). WT mice present 98.4% normal glomeruli (**Supplementary Figure 1A&B**). Although the number of healthy glomeruli is noticeably higher in KO transplanted with WT bone marrow (**Supplementary Figure 1A-C**), glomerular damage appears reduced in KO transplanted with KO bone marrow (29.6 ± 9.0% of normal glomeruli) in comparison to natural COL4A3KO mice (15.6 ± 2.6%), suggesting irradiation of the recipient mice provides some histological improvement. The difference in percent normal glomeruli between KO transplanted with COL4A3 KO bone marrow and KO was not statistically significant (p=0.06). WT mice present with 6.0 ± 0.5% of percent relative interstitial volume and 0.2 ± 0.4% of percent tubular atrophy whereas KO mice present with markedly increased values, with 54.6 ± 2.2% and 79.1 ± 2.2% of percent relative interstitial volume and percent tubular atrophy, respectively (**Supplementary Figure 1C-E**). Significant improvement was observed in both percent relative interstitial volume and percent tubular atrophy in COL4A3 KO mice rescued with WT bone marrow (19.7 ± 1.5% and 28.4 ± 6.4%) when compared with mice rescued with KO bone marrow (41.4 ± 4.0% and 62.4 ± 7.2%), or in comparison to untreated COL4A3 KO mice (54.6 ± 2.2% and 79.1 ± 2.2%) (**Supplementary Figure 1D&E**). Percent relative interstitial volume and percent tubular atrophy decrease (although not statistically significant) in irradiated COL4A3 KO mice rescued with COL4A3 KO bone marrow, when compared with untreated COL4A3 KO mice.

The histological improvement in the COL4A3 KO mice transplanted with WT bone marrow is associated with *de novo* expression of α3(IV) collagen in the GBM (**Supplementary Figure 1F**). Expression of α3(IV) collagen was not detected in KO and KO transplanted with KO bone marrow , providing further evidence that the WT bone marrow-derived cells provide COL4A3 KO recipients with the missing chain of type IV collagen. Furthermore, a marked increase in GBM expression of α5(IV) collagen is noted in the KO transplanted with WT bone marrow when compared to KO and KO transplanted with KO bone marrow (**Supplementary Figure 1F**). Our immunostaining results also reveal basal expression of α5(IV) in KO and KO transplanted with KO bone marrow, corroborating previous findings(6, 9). The marked increase of α5(IV) collagen, associated with *de novo* α3(IV) expression in KO transplanted with WT bone marrow, is evidence for a change in type IV collagen GBM protomer composition following treatment with WT bone marrow cells.

Syngeneic and non-syngeneic bone marrow transplantation improves proteinuria and provides the missing chain of type IV collagen in COL4A3 KO mice on the 129Sv genetic background.

We evaluated whether COL4A3 KO mice on the 129Sv genetic background (129KO) could benefit from syngeneic bone marrow transplant therapy and whether renal phenotypic improvement is possible following non-syngeneic bone marrow transplantation. In this study, COL4A3 KO mice on the 129Sv genetic background were

transplanted using bone marrow cells from WT mice and COL4A3KO mice on 129Sv and C57BL/6 genetic backgrounds (**Supplementary Figure 2A**). Our results indicate that WT bone marrow cells significantly improve the renal disease in transplanted COL4A3 KO recipient mice on 129Sv genetic background, in contrast with COL4A3 KO recipients transplanted with COL4A3 KO bone marrow. In our experiment, 129KO transplanted with 129 WT bone marrow present with improved urine albumin/urine creatinine ratio (16.7 ± 10.16) in contrast to 129KO transplanted with 129 KO bone marrow (44.3 ± 1.3) (**Supplementary Figure 2B**). Also, in contrast with 129KO transplanted with 129 KO bone marrow, which appear cachexic, 129KO transplanted with 129 WT bone marrow appear healthier and were more active (data not shown). In both COL4A3KO on the C57BL/6 genetic background transplanted with C57BL/6 WT bone marrow and 129KO transplanted with 129 WT bone marrow, α3(IV) NC1 domain was detected by western blot analyses, whereas no expression was detected in COL4A3KO on C57BL/6 genetic background transplanted with C57BL/6 COL4A3KO bone marrow and 129KO transplanted with 129 KO bone marrow (**Supplementary Figure 2C**). Furthermore, 129KO transplanted with 129 WT bone marrow, live up to nearly 16 weeks of age, whereas all 129KO transplanted with 129 KO bone marrow died from renal failure at 8 weeks of age (**Supplementary Figure 2E**). These results contrast those reported by Katayama et al(8): COL4A3 KO mice on the 129Sv genetic background transplanted with WT BM from 129Sv syngeneic donors showed renal phenotypic improvement associated with type IV collagen α3-chain GBM deposition similar to that observed in C57BL/6 syngeneic BMT in our previous study(22). Furthermore, to test whether irradiation alone would provide a survival advantage in

COL4A3 KO mice on the 129Sv genetic background (129KO), we irradiated 5-weeks old 129KO with a single total body irradiation exposure to 600rads (n=4), and compared length of survival to non-irradiated 129KO animals (n=4). All animals died from renal failure at 10 weeks of age, 5 weeks post irradiation, indicating that in our laboratory, irradiation alone did not increase survival in COL4A3 KO mice on the 129Sv genetic background (data not shown).

In non-syngeneic bone marrow transplanted animals, COL4A3 KO mice on the 129Sv genetic background transplanted with C57BL/6 WT and C57BL/6 COL4A3 KO unfractionated bone marrow cells (**Supplementary Figure 2A**), the 129KO transplanted with C57BL/6 WT unfractionated bone marrow cells showed a dramatic improvement in overall appearance, gait, and body weight (15.1g ± 1) in contrast with 129KO transplanted with C57BL/6 COL4A3 KO unfractionated bone marrow cells (12.8g ± 0.1) (data not shown and **Supplementary Figure 2D**), associated with improved proteinuria (C57BL/6 WT transplant: 45 ± 7.8, in contrast to C57BL/6 KO transplant: 76 ± 8.8) (**Supplementary Figure 2B**). Collectively, our results show that in both syngeneic and non-syngeneic bone marrow transplanted mice on the 129Sv genetic background, improvement in the renal phenotype is associated with a cell providing the wild-type allele of the COL4A3 gene.

A single injection with undifferentiated WT bone marrow cells in COL4A3 KO mice provides the missing chain of type IV collagen in kidney GBM

Multiple infusions of WT bone marrow in COL4A3 KO mice on the C57BL/6 genetic background in late stages of the renal disease (20 weeks-old) showed statistically significant improvement in the renal phenotype associated with α3(IV) GBM deposition (**Figure 1**). We then asked whether a single injection of WT bone marrow cells in COL4A3 KO mice at 8 weeks of age (onset of the renal disease in the C57BL/6 genetic background) could rescue the renal phenotype (**Supplementary Figure 3A**). Urine albumin/urine creatinine ratio measurements indicate that COL4A3 KO mice treated with WT bone marrow present improved proteinuria, although non-statistically significant (p=0.11)-(45.9 ± 12.8) in comparison to COL4A3 KO mice treated with KO bone marrow (90.5 ± 19.0) (data not shown). Furthermore, RT PCR amplification of COL4A3 transcript revealed expression of the missing gene in kidney cDNA from WT and KO injected with WT bone marrow cells , but no expression was detected in control kidney cDNA from KO and KO injected with KO bone marrow cells (**Supplementary Figure 3B**). Finally, western blot analyses of kidney ECM proteins reveal α3(IV) NC1 in KO injected with WT bone marrow cells whereas no α3(IV) NC1 was detected in KO injected with KO bone marrow cells (**Supplementary Figure 3C**). Together, these results suggest that a single injection of undifferentiated WT bone marrow in COL4A3 KO mice provides the missing chain of type IV collagen in these mice.

Lymphocytes and monocytes/macrophages are not required for the emergence of the missing chain of type IV collagen in COL4A3 KO mice

Our results indicate that circulating bone marrow derived cells provide a therapeutic benefit in COL4A3 KO mice. Next, we tested the hypothesis that such therapeutic cells may derive from the hematopoietic compartment of the bone marrow. A previous study using bone marrow-derived mesenchymal stem cells (MSCs) in COL4A3 KO mice suggested that MSCs cellular therapy did not lend itself to the synthesis of the missing chain of type IV collagen(15); therefore, we focused our attention on the hematopoietic compartment. The COL4A3 KO kidney disease involves a considerable amount of immune infiltration, which possibly plays a critical role in glomerular crescent formation(5, 10, 14, 16, 19, 21, 23, 24). We asked specifically whether lymphocytes and macrophages are among the therapeutic cells in the cell-based therapy in COL4A3 KO mice. For these experiments, we employed Rag-1KO(12) and CD11bKO(11) mouse models, lacking mature lymphocytic cells and monocyte/macrophages, respectively. We previously demonstrated the role of B- and T-lymphocytes by crossing COL4A3 KO mice onto the immunodeficient Rag-1KO background. Our results demonstrate that B- and T-lymphocytes are not required for the glomerulonephritis but are essential components of tubulo-interstitial inflammation and fibrosis(10), and genetic deletion of B- and T-lympocytes in COL4A3 KO mice did not improve survival (**Supplementary Figure 7Q**). Similarly, reduction of interstitial and glomerular macrophages did not ameliorate the renal pathology in COL4A3KO mice(2). We transplanted the COL4A3 KO mice with bone marrow harvested from Rag-1KO and CD11bKO animals in order to ablate specific cell sub-populations from the hematopoietic compartment of the bone marrow (Supplementary **Figure 4A**). Twelve weeks following the transplant, we analyzed the genotype of the bone marrow in the transplanted animals. In both

experimental groups, we detected both wild-type and KO alleles for the Rag-1 and CD11b mutations (Supplementary **Figure 4B&C**). The chimeric genotype of the bone marrow indicated that not all B-, T-lymphocytes, monocytes/macrophages in COL4A3KO transplanted with Rag1 KO bone marrow and COL4A3KO transplanted with CD11b KO bone marrow are ablated. The number of $CD19^+$ cells (lymphocytes) in the kidney of the KO transplanted with Rag1 KO bone marrow was greatly reduced, and we did not detect $CD11b^+$ cells in the kidneys of COL4A3 KO transplanted with CD11b KO bone marrow (Supplementary **Figure 4D-J**). The analysis of the kidney disease progression in COL4A3 KO transplanted with CD11b KO bone marrow and COL4A3 KO transplanted with Rag1 KO bone marrow reveal a mild decrease in proteinuria (Supplementary **Figure 4K, Supplementary Table 1**), and a statistically significant improvement in renal histology, similar to that observed in COL4A3 KO mice transplanted with wild-type bone marrow (Supplementary **Figure 4L-N, SupplementaryTable 1**). Based on our assessment of histological findings, the decreased number of B- and T-lymphocytes and monocyte/macrophages in the renal infiltrate of COL4A3 KO mice did not affect the renal disease progression, and both COL4A3 KO transplanted with Rag1 KO bone marrow and COL4A3 KO transplanted with CD11b KO bone marrow present with a similar phenotypic improvement as observed in COL4A3 KO transplanted with WT bone marrow, in contrast with COL4A3 KO transplanted with COL4A3 KO bone marrow (Supplementary **Figure 4M&N, Supplementary Table 1)**. Furthermore, we detected the expression of the missing chain of type IV collagen in WT, COL4A3 KO transplanted with Rag1 KO bone marrow and COL4A3 KO transplanted with CD11b KO bone marrow, but not in COL4A3 KO ^{BMT}

^{COL4A3KO} control mice (Supplementary **Figure 4O**), indicating that B-/T-lymphocytes and monocytes/macrophages are not required for the emergence of the missing α3(IV) in the GBM of bone marrow transplanted COL4A3 KO mice.

Mouse embryonic stem cells infusion leads to improved renal function and kidney histology in COL4A3 KO mice, provide type IV collagen α3 and α5 chains, and improve GBM architecture in COL4A3 KO mice

Undifferentiated mouse embryonic stem cells (mESCs) ($1x10^6$) were administered systematically into 8 weeks-old COL4A3 KO (Supplementary **Figure 5A**). Injection of these cells via retro-orbital plexus route led to occasional formation of a cell mass at the injection site, which did not impair the ability to determine the capacity of these cells in reversing renal defects. Urine protein excretion (Supplementary **Figure 5B**) and BUN (Supplementary **Figure 5C**) measurements demonstrated a significant improvement in COL4A3 KO mice treated with mESCs in comparison with untreated COL4A3 KO mice (Supplementary **Table 1**). Histological findings indicated that kidney damage is significantly reversed upon mESCs treatment (Supplementary **Figure 5D-G**), resulting in an increased fraction of normal glomeruli (Supplementary **Figure 5E**) and significantly improved tubulo-interstitial compartment. Morphometric analyses revealed that the COL4A3 KO mice injected with mESCs exhibit a significant decrease in interstitial volume and tubular atrophy at 21 weeks of age (Supplementary **Figure 5F&G,** Supplementary **Table 1**).

Administration of GFP^+ mESCs at 8 weeks of age leads to the emergence of GFP^+ cells in the glomeruli by 12.5 and 21 weeks of age (Supplementary **Figure 5H-K**). Glomerular morphometric analysis demonstrates that in KO injected with mESCs about 4.3 ± 0.6 % of the resident glomerular cells are stem cell-derived at 21 weeks of age, 13 weeks after mESCs injection (Supplementary **Figure 5K**). Recruitment of male derived mESCs to the glomeruli of female recipient mice was also demonstrated by Y-chromosome staining (Supplementary **Figure 5L&M**). Furthermore, GFP^+ cells co-localized with nephrin labeling (specific to podocytes) (Supplementary **Figure 5J&N**), suggesting that the mESCs recruited into the glomeruli acquire expression of podocyte specific marker. Several studies suggest that podocytes and glomerular endothelial cells produce type IV collagen α3 chain (4, 22). Immunofluorescence experiments using chain specific type IV collagen antibodies, described in previous publications(17, 22), were performed to evaluate deposition of α3 and α5(IV) collagen chains in the GBM of KO injected with mESCs. Immunostaining of kidney sections from KO injected with mESCs reveals a patchy and speckled linear labeling pattern for α3 chain and a significant recovery of α5 chain expression in the GBM (Supplementary **Figure 5O-T**).

Western blot analyses of renal basement membrane proteins reveal *de novo* expression of α3 and α4 chains type IV collagen in kidney sections of KO mice injected with mESCs (Supplementary **Figure 6C**). To evaluate whether the newly attained type IV collagen α3 chain protein expression led to appropriate α3 chain incorporation into the type IV collagen network and re-induced the incorporation of α4 and α5 chains, renal basement membranes from snap frozen kidneys of WT, COL4A3 KO control, and KO injected with mESCs were isolated using salt and detergent extraction, as previously

described(22). To liberate the non-collagenous domains, the cell free basement membrane extract was subsequently subjected to collagenase digestion to degrade triple helical collagen networks (Supplementary **Figure 6A-E**). Among the resulting protein mixture is the C-terminal globular hexamer, which represents assembled type IV collagen protomers. Immunoblotting with α3 antibodies reveals the presence of α3NC1 collagen chain in the hexamers of control mice and KO injected with mESCs but not in KO control mice (Supplementary **Figure 6C**). The α3(IV) NC1 could also be detected as dimers and monomers in KO injected with mESCs, similar to control WT mice (Supplementary **Figure 6C**). Disulfide-bond-reducing SDS-PAGE analysis revealed that such α3 chain expression in the GBM type IV collagen network was associated with the re-emergence of α4(IV) NC1 protein expression in the type IV collagen NC1 hexamers, when compared to COL4A3 KO mice (Supplementary **Figure 6C**). The C-terminal NC1 domain of type IV collagen chains likely plays a key role in the molecular recognition and assembly of type IV collagen protomers and hexamers (1, 18, 20). The incorporation of the newly expressed α3 chain into the type IV collagen network upon stem cell administration was further confirmed by immunoprecipitation of α3NC1 containing hexamers using the anti-α3NC1 antibody. Immunoblotting of precipitated α3NC1 containing hexamers, the α4 and α5 chains could be detected in the precipitated hexamers of WT control mice and in COL4A3 KO injected with mESCs, but not in the COL4A3 KO mice (Supplementary **Figure 6F**). No such interaction was found when an anti-FLAG antibody used in the immunoprecipitation experiments (**Supplemental figure 8**). In addition, our studies using human embryonic stem cells (hESCs) in COL4A3/Rag-1 DKO mice demonstrate expression of the missing chain of type IV collagen

(**Supplemental figure 7 O&P**), provided by hESCs incorporated within the mouse GBM type IV collagen composition, corroborating previous work in which the human α-chain of type IV collagen in COL4A3 KO mice can assemble and form a chimeric protomer(3).

Electron microscopy (EM) analyses were performed to examine kidney tissues at 12.5 and 21 weeks of age with particular emphasis on GBM architecture and podocyte integrity. Podocytes from COL4A3 KO mice show foot process effacement (flattening) and microvillous transformation using scanning EM (SEM), when compared to WT control mice (Supplementary **Figure 6G-I**). Transmission EM analysis (TEM) of wild-type mice shows normal GBM pattern (Supplementary **Figure 6J&M**). COL4A3 KO mice at 8 weeks, 12.5 weeks and 21 weeks reveal GBM damage with characteristic splitting, multi-laminations, thinning and thickening, as observed in human Alport syndrome (7) (Supplementary **Figure 6K&N**). KO mice injected with mESCs exhibit significant GBM repair at 21 weeks of age (13 weeks after injection) with significant repair of podocyte integrity with reduction in foot processes effacement (Supplementary **Figure 6L&O**).

Differentiated mESCs and podocytes do not rescue the renal phenotype in COL4A3 KO mice

We next aimed to characterize whether differentiated mESCs and cultured podocytes could restore renal functions in COL4A3 KO mice (**Supplemental Figure 7A&B**). We used mESCs which constitutively express GFP, yet we failed to detect GFP labeling in

COL4A3 KO mice treated with differentiated mESCs (**Supplemental Figure 7D&E**). The podocyte cell line used was previously characterized (13). To generate the line, mouse podocytes were transfected with Simian Virus 40 (SV40) T-Ag (**Supplemental Figure 7F**). We failed to detect SV40 T-Ag positive cells in COL4A3 KO mice treated with podocytes (**Supplemental Figure 7G**). These results suggest that these cells did not home to the kidney glomeruli. No α3(IV) chain was detected in the glomeruli of COL4A3 KO mice treated with differentiated mESCs or podocytes (**Supplemental Figure 7H-J**). In contrast with KO mice treated with mESCs, no improvement in urine albumin/urine creatinine ratio was observed in KO mice treated with podocytes and KO mice treated with differentiated mESCs 4.5 weeks post treatment (WT: 0.5 ± 0.1, COL4A3 KO: 12.2 ± 3.7, KO treated with mESCs: 2.2 ± 0.2, KO treated with differentiated mESCs: 15.53 +/- 5.0, KO treated with podocytes: 10.0 +/- 4.4, **Supplementary Figure 7C**). Finally, in contrast with KO treated with mESCs, (Supplementary **Figure 5L&M**), Y-chromosome labeling for mESCs showed no homing of differentiated mESCs to the kidney glomeruli of COL4A3 KO (**Supplementary Figure 7K-M**). These results indicate that podocytes and differentiated mESCs did not provide the missing chain of type IV collagen to the diseased glomeruli.

Supplementary Materials and Methods:

Genotyping and bone marrow genomic DNA PCR

To genotype COL4A3 KO mice, genomic DNA from tail snips or bone marrow flushed from tibia and femur was purified using Quiagen DNeasy® Blood and Tissue total DNA purification kit according to the manufacturer's directions. The genotyping PCR

employed the following primers: 5' TTCCCCTGTCACCAGGATTTCCC-3' (wild-type allele primer), 5'-ACGACCTTTCTTAAACTAGAAGAAGTC-3' (common primer), and 5'-TGCTAAAGCGCATGCTCCAGACTGC-3' (knockout allele primer). The master mixes contained the common primer and either of the wild-type or knockout allele primers. The PCR reaction was run with the following conditions: 35 repeats of [95°C for 40s, 65°C for 40s, and 72°C for 3 minutes]. The PCR products were migrated by gel electrophoresis on a 1% agarose gel in 1X Tris-acetate-ethylenediamine tetraacetic acid (EDTA) buffer (TAE buffer). The 1000bp product was amplified from the wild-type allele, and the 850bp product was amplified from the knockout allele. Genotyping for Rag-1 KO mice requires 3 primers: 3'-TTGGATGTGGAAGGGCGAG-5', 3'-GAGGTTCCGCTAGCACTCTG-5', and 3'-CCGGACAAGTTTTTCATCGT-5'. PCR amplification of tail snip genomic DNA using these primers with the following conditions 35x[95C for 30s, 58C for 40s, 72C for 45s] and gel electrophoresis allowed for the visualization of the PCR products, with a 474bp wild-type fragment, and 530bp knockout fragment. Genotyping for CD11b KO requires 3 primers: 3'-ATCGCCTTCTTGACGAGTTC-5', 3'-TAGGCTATCCAGAGGTAGAC -5', and 3'-CATACCTGTGACCAGAAGAGC -5'. PCR amplification of tail snip genomic DNA using these primers with the following conditions 35x[95C for 30s, 56C for 1min, 72C for 1min] and gel electrophoresis allowed for the visualization of the PCR products, with a 300bp wild-type fragment, and 600bp knockout fragment.

Supplementary Figure Legend

Supplementary Figure 1. Histological findings of WT and COL4A3 KO bone marrow transplanted COL4A3 KO mice and immunostaining for α3 and α5(IV) collagen

A. Representative PAS staining of glomeruli from 21 weeks-old WT, KO, KO mice transplanted with COL4A3 KO bone marrow and KO mice transplanted with WT bone marrow , 400X, and **B** morphometric analyses of percent normal glomeruli. **C**. Representative H&E staining of the kidney cortex of 21 weeks-old KO mice transplanted with COL4A3 KO bone marrow and KO mice transplanted with WT bone marrow , with black arrow heads pointing to globally sclerosed glomeruli and green arrow heads pointing to normal healthy glomeruli, 100X. **D-E** Morphometric analyses of percent relative interstitial volume (**D**), and percent tubular atrophy (**E**). Number of mice: WT (n=5), COL4A3 KO (n=5), KO transplanted with COL4A3 KO bone marrow (n=3), and KO mice transplanted with WT bone marrow (n=5). Mice are 21 weeks-old. **F**. Immunolabeling of mouse α3 and α5(IV) collagen NC1 domain in WT, KO, KO mice transplanted with COL4A3 KO bone marrow and KO mice transplanted with WT bone marrow. All mice are 21 weeks-old, 400X. * $p<0.05$, ** $p<0.01$

Supplementary Figure 2. Bone marrow transplant studies in 129Sv and C57BL/6 COL4A3 KO mice

A. Schematic representation of experimental set up: COL4A3 KO mice on the 129Sv genetic background were transplanted with 129Sv COL4A3 KO (n=4), WT (n=6), C57BL/6 COL4A3 KO (n=4), and WT (n=4) bone marrow. **B.** Urine albumin/urine creatinine ratio depicts that 129KO mice transplanted with 129 WT bone marrow and

129KO mice transplanted with C57BL/6 WT bone marrow , in contrast with 129KO mice transplanted with 129 KO bone marrow and 129KO mice transplanted with C57BL/6 KO bone marrow, present with significant improvement in proteinuria. **C**. Western blot analyses for α3(IV) expression in kidney extracellular matrix protein for all experimental groups **D.** Weight loss in male 129KO animals transplanted with C57BL/6 KO bone marrow (n=4) in comparison to male 129KO animals transplanted with C57BL/6 WT bone marrow (n=4). **E**. Survival curve comparing 129KO transplanted with 129 WT bone marrow (n=3) and 129KO transplanted with C57BL/6 KO bone marrow (n=4) * $p<0.05$, ** $p<0.01$

Supplementary Figure 3. Single bone marrow cell injection and parabiotic pairing in C57BL/6 COL4A3 KO mice provide α3(IV) chain to the GBM

A. Schematic representation of experimental set up: a single bone marrow (BM) infusion from COL4A3 KO donor into 8-weeks old COL4A3 KO recipients (n=4) and WT donor into COL4A3 KO littermate recipients (n=4). The mice were then euthanized at 20 weeks of age. **B**. RT-PCR analyses for expression of COL4A3 and β-actin control and **C.** western blot immunolabeling for mouse α3(IV) in kidneys from WT, KO mice infused with KO bone marrow and KO mice infused with KO bone marrow. **D**. Survival curve comparing C57BL/6 COL4A3 KO mice infused with C57BL/6 COL4A3 KO (KO $^{BMi\ KO}$, n=5) or WT (KO $^{BMi\ WT}$, n=5) bone marrow. Arrows represent the number of bone marrow infusions at the indicated time on the x-axis. T: the experiment was terminated and all animals were euthanized. **E**. Schematic representation of experimental set up of

parabiotic pairing of WT and COL4A3 KO mice at 5 weeks of age. The parabionts were then euthanized 6 weeks post joining and **F.** western blot immunolabeling for mouse α3(IV) in each parabiont (pWT and pKO) revealed that long-term blood exchange allows for α3(IV) chain expression in the GBM of the COLA3 KO recipient.

Supplementary Figure 4. Lymphocytes and macrophages are not required for the cell-based therapy in COL4A3 KO mice

A. Schematic of the experimental set up: C57BL/6 COL4A3 KO mice were transplanted with bone marrow harvested from Rag-1 KO and CD11b KO donors. **B**. Rag-1 genotyping PCR on genomic DNA harvested from the bone marrow of COL4A3 KO mice transplanted with Rag-1 KO bone marrow **C**. CD11b genotyping PCR on genomic DNA harvested from the bone marrow of COL4A3 KO mice transplanted with CD11b KO bone marrow **D-F** Immuunohistochemisry for podocin (green) and CD19 (red) expression in the kidneys of COL4A3 KO, Rag-1 KO and COL4A3 KO mice transplanted with Rag-1 KO bone marrow, **G** secondary antibody only negative control (glomeruli are circled), and **H-J** immuunohistochemisry for podocin (green) and CD11b (red) expression in the kidneys of COL4A3 KO, CD11bKO and COL4A3 KO mice transplanted with CD11b KO bone marrow. **K.** Urine albumin/urine creatinine measurement in COL4A3 KO transplanted with WT bone marrow, COL4A3 KO, COL4A3 KO transplanted with Rag-1 KO bone marrow and COL4A3 KO mice transplanted with CD11b KO bone marrow. **L.** Representative PAS staining of kidneys from COL4A3 KO mice transplanted with WT bone marrow, COL4A3 KO mice

transplanted with COL4A3 KO bone marrow, COL4A3 KO mice transplanted with Rag-1 KO bone marrow and COL4A3 KO mice transplanted with CD11b KO bone marrow (100X), and **M-N** morphometric analysis of percent normal glomeruli and percent tubular atrophy. **O**. Western blot analyses of kidney extracellular matrix proteins harvested from WT, COL4A3KO mice transplanted with COL4A3 KO bone marrow, COL4A3KO mice transplanted with Rag-1 KO bone marrow, and COL4A3KO transplanted with CD11b KO bone marrow mice, indicating α3(IV) collagen chain is expressed in WT, COL4A3KO mice transplanted with Rag-1 KO bone marrow, and COL4A3KO transplanted with CD11b KO bone marrow, but not in COL4A3KO mice transplanted with COL4A3 KO bone marrow (control).

Supplementary Figure 5. mESCs rescue COL4A3 KO renal phenotype

A. Schematic representation of experimental set up: 8 and 13 weeks-old COL4A3 KO and WT mice received mESCs (8 weeks-old COL4A3 KO recipients: n=6; 13 weeks-old COL4A3 KO recipients: n=4; 8 weeks-old WT recipients: n=3), 8weeks-old COL4A3KO mice received vehicle (n=6) **B**. Urine albumin/urine creatinine ratio in 12 and 21 weeks-old WT, COL4A3 KO, and COL4A3 KO injected with mESCs. **C.** Blood Urea Nitrogen (BUN) in 12 (for mice injected at 8 weeks of age) and 21 (for mice injected at 13 weeks of age) weeks-old WT, COL4A3 KO, and KO injected with mESCs. **D**. Representative H&E pictures at 400X (upper panel) and 200X (lower panel) of kidneys from 21 weeks-old WT, COL4A3 KO, and KO injected with mESCs and morphometric analyses of **E**.

percent normal glomeruli, **F**. percent interstitial volume, and **G**. percent tubular atrophy. **H-J** GFP labeling of kidney glomeruli: while WT (**H**) and COL4A3 KO (**I**) mice did not show any GFP labeling, KO mice injected with mESCs revealed positive GFP labeling in the glomeruli (**J**). **K.** Quantitation of GFP positive cells revealed 4.3 ± 0.6% GFP^+ cells per glomerulus in 21 weeks-old KO mice injected with mESCs (n=2) in comparison to WT mice injected with mESCs (0.5 ± 0.2%, n=3). **L-M.** Y-chromosome labeling shows positive staining in mESCs colony (**L**) and in KO mice injected with mESCs (**M**). **J-N** Co-localization of GFP labeling with the podocyte specific marker nephrin in glomeruli of KO mice injected with mESCs . **O-T** Immunofluorescence analysis of type IV collagen α3 (**O-Q**) and α5 (**R-T**) chain expression in WT, COL4A3 KO and KO injected with mESCs depicts reemergence of GBM α3 and α5 chains in glomeruli of KO mice injected with mESCs. * $p<0.05$

Supplementary Figure 6. mESCs restore α3α4α5(IV) protomer composition in the GBM of COL4A3 KO mice

A-B Schematic illustration of NC1 hexamer populations in GBM. Each oval represents a single type IV collagen α chain NC1 domain from collagenase solubilized GBM from WT and COL4A3 KO control mice, KO mice injected with mESCs. **C.** Western blot analysis of native type IV collagen α3NC1 domains. Naive type IV collagen hexamers in WT and KO mice injected with mESCs (at 12.5 and 21 weeks of age) contain α3-chain, but no α3 NC1 was detected in COL4A3 KO control mice. Type IV collagen α3 dimers and α3 and α4 monomers (28 kDa) could be detected in WT and KO mice injected with mESCs at 12.5 and 21 weeks, but not in COL4A3 KO control mice. Δ: degradation

product **D-F** Immunoprecipitation (IP) of α3, α4 and α5 containing NC1 hexamers from collagenase-solubilized GBM by α3 antibody. Anti-α3 antibody was used to immunoprecipitate α3NC1 containing hexamers from collagenase solubilized GBM from WT control mice and KO mice injected with mESCs. α3**,** α4 and α5NC1 monomers and dimers can be detected in precipitated α3NC1-hexamers of WT mice and KO mice injected with mESCs at 12.5 (left panel) and 21 (middle panel) weeks of age. Δ: degradation product. **H-P** Ultrastructural Analysis of Glomerular Basement Membrane (GBM) of mice at 21 weeks of age. Scanning electron microscopy (SEM). **H.** Normal WT mice show a complex interdigitation (arrows) of podocyte foot processes between adjacent podocytes forming the filtration barrier. **I.** In COL4A3 KO mice the interdigitation of foot processes is lost (arrows) and forms sheet like structures. **J.** Treatment of COL4A3 KO mice with mESCs recovers foot process interdigitation (Magnification: x15,000). **K-P.** Transmission electron microscopy (TEM). **K.** 21 week-old WT mice show normal GBM structure (dashed line in **K**, arrows in **N**). Between the foot processes the slit diaphragm can be seen (**N**). At low (**L**) and high (**O**) magnification the GBM of untreated COL4A3 KO mice shows splitting and basket-weave appearance (arrows in **O**), lamination and thinning (dashed line in **L**). Podocytes show microvillous transformation and foot process effacement. **M**. Treatment of COL4A3 KO mice with mESCs inhibits foot process effacement and reconstitutes damaged GBM structure (dashed line in **M**, arrows in **P**).

Supplementary Figure 7. Differentiated mESCs and podocytes do not rescue the renal phenotype in COL4A3 KO mice

A. Schematic representation of differentiated mESCs (n=5) and **B**. podocyte cell injection in 8 weeks-old C57BL/6 COL4A3 KO mice (n=4). **C.** Urine albumin/urine creatinine ratio measurements in WT (n=3), COL4A3 KO (n=6), KO injected with mESCs(n=6), KO injected with differentiated mESCs (n=5), and KO injected with podocytes (n=4). **D.** GFP expression in dispersed mESCs and **E**. immunolabeling for GFP expression in glomeruli of COL4A3 KO mice treated with differentiated mESCs. **F.** SV40 T-Ag labeling in culture podocytes and **G**. SV40 T-Ag labeling in glomeruli of COL4A3 KO mice treated with podocytes. **H-J** Immunolabeling for α3(IV) chain in glomeruli of WT (**H**), KO injected with differentiated mESCs (**I**), and KO injected with podocytes (**J**). **K-M**. Y-chromosome labeling in glomeruli of female WT mice (negative control), of male WT mice (positive control, arrows point to Y-chromosome), and of female KO mice injected with differentiated mESCs. **N.** Podocytes cultured under permissive conditions (Collagen I coated surface, no γ-interferon, 37C) are positively immunolabeled with podocyte markers nephrin and podocin. mESCs allowed to differentiated as EBs for 5 days without LIF and plated onto collagen IV coated surface are also positively immunolabeled for nephrin and podocin. **O.** Experimental set up: 8 weeks-old COL4A3/Rag-1 double KO mice received hESCs (n=7), all mice were sacrificed at 21 weeks of age. **P**. α3 chain of type IV collagen was also detected in Rag-1 KO mice, Rag-1 KO mice treated with hESCs, COL4A3/Rag-1 double KO mice treated with hESCs, and human sample, but not in COL4A3/Rag-1 double KO mice treated with vehicle (PBS). **Q**. Survival curve comparing COL4A3 KO and COL4A3/Rag-1 double KO mice. ** $p<0.01$

Supplementary Figure 8. Coomassie blue staining of western blot PVDF membranes

Western blot membranes were stained with coomassie blue dye to assess equal protein concentration. Experiment and figure are indicated below each membrane.

Supplementary Table 1. Morphometric analyses and renal function tests ([a]P < 0.05, [b]P < 0.01)

Bone marrow infusion (Figure 1)				
	Urine albumin/creatinine			
	20 weeks	21 weeks	22 weeks	23 weeks
KO + WT BM	36.6 ± 12.0	28.8 ± 4.5	44.2 ± 9.5	54.2 ± 11.2
KO + KO BM	44.0 ± 3.2	84.0 ± 23.3	99.6 ± 8.1	94.3 ± 22.9
Statistical significance	No	a	b	p=0.2
	Morphometric analyses			
	Normal glomeruli	Glomerular sclerosis	Tubular atrophy	Relative interstitial volume
KO + WT BM	22.3 ± 0.4%	70.9 ± 3.4%	44.4 ± 3.6%	30.3 ± 2.5%
KO + KO BM	6.5 ± 0.9%	80.0 ± 2.7%	82.1 ± 1.6%	56.4 ± 2.8%
Statistical significance	p=0.07	a	b	b

Blood transfusion (Figure 2)					
	Morphometric analyses			Renal Function tests	
	Normal glomeruli	Tubular atrophy	Relative interstitial volume	Serum BUN	Urine albumin/creatinine
WT	99.6 ± 0.4%	0.1 ± 0.1%	6.6 ± 0.3%	22.5 ± 6.5 mg/dl	0.5 ± 0.1
KO at 12.5 wk	75.8 ± 4.5%	22.6 ± 6.4%	16.1 ± 2%	51 ± 15.1 mg/dl	12.2 ± 3.7
KO + 8 wk transfusion	97.7 ± 1.2%	5.4 ± 3.0%	9 ± 2.4%	29.9 ± 2.9 mg/dl	2.5 ± 0.9
Statistical significance	a	a	a	a	a
WT	98.9 ± 0.3%	0.1 ± 0.1%	6.9 ± 0.6%	33.5 ± 2.9 mg/dl	1.5 ± 0.8
KO	22.4 ± 4.1%	77.3 ± 5.2%	33.4 ± 3.2%	316 ± 19.9 mg/dl	25.8 ± 3.9
KO + 23wk KO transfusion	20.3 ± 6.8%	92.6 ± 1.7%	31.8 ± 4.7%	363 ± 3.9 mg/dl	22.6 ± 2.7
KO + 23wk WT transfusion	36.3 ± 8.7%	19.2 ± 3.9%	16.9 ± 5.18%	203 ± 60.2 mg/dl	17.3 ± 3.8
Statistical significance	a	a	a	a	No

Bone marrow transplant studies (Supplementary Figure 4)			
	Urine	Morphometric analyses	
	albumin/creatinin	Normal glomeruli	Tubular atrophy
COL4A3KO + WT BMT	21.2 ± 4.5	47.5 ± 6.5%	43.6 ± 1.9%
COL4A3KO	33.6 ± 3.0	32.1 ± 3.8%	60.5 ± 1.1%
COL4A3KO + Rag-1 KO BMT	27.4 ± 8.0	48.4 ± 7.2%	32.8 ± 3.3%
COL4A3KO + CD11b KO BMT	23.9 ± 9.8	62.2 ± 3.2%	32.1 ± 1.9%
Statistical significance	No	a	a

mESCs studies (Supplementary Figure 5)			
	Urine albumin/creatinine		BUN
	12 weeks	21 weeks	
WT	0.5 ± 0.08	1.5 ± 0.8	49.2 ± 3.6
KO	12.2 ± 3.7	25.8 ± 3.9	316.7 ± 19.9
KO + mESCs	2.2 ± 0.2	7.4 ± 2.1	112.7 ± 1.2
Statistical significance	a	a	a
	Morphometric analyses		
	Normal glomeruli	Tubular atrophy	Relative interstitial volume
WT	98.9 ± 0.3%	0.1 ± 0.1%	6.9 ± 0.6%
KO	22.4 ± 4.1%	77.3 ± 5.2%	33.4 ± 3.2%
KO + mESCs	44.7 ± 19.9%	23 ± 4%	23.9 ± 3.6%
Statistical significance	a	a	a

References (Supplementary text):

1. **Borza DB, Bondar O, Ninomiya Y, Sado Y, Naito I, Todd P, and Hudson BG.** The NC1 domain of collagen IV encodes a novel network composed of the alpha 1, alpha 2, alpha 5, and alpha 6 chains in smooth muscle basement membranes. *J Biol Chem* 276: 28532-28540, 2001.
2. **Clauss S, Gross O, Kulkarni O, Avila-Ferrufino A, Radomska E, Segerer S, Eulberg D, Klussmann S, and Anders HJ.** Ccl2/Mcp-1 blockade reduces glomerular and interstitial macrophages but does not ameliorate renal pathology in collagen4A3-deficient mice with autosomal recessive Alport nephropathy. *J Pathol*, 2008.
3. **Heidet L, Borza DB, Jouin M, Sich M, Mattei MG, Sado Y, Hudson BG, Hastie N, Antignac C, and Gubler MC.** A human-mouse chimera of the alpha3alpha4alpha5(IV) collagen protomer rescues the renal phenotype in Col4a3-/- Alport mice. *Am J Pathol* 163: 1633-1644, 2003.
4. **Heidet L, Cai Y, Guicharnaud L, Antignac C, and Gubler MC.** Glomerular expression of type IV collagen chains in normal and X-linked Alport syndrome kidneys. *Am J Pathol* 156: 1901-1910, 2000.
5. **Huang XR, Tipping PG, Apostolopoulos J, Oettinger C, D'Souza M, Milton G, and Holdsworth SR.** Mechanisms of T cell-induced glomerular injury in anti-glomerular basement membrane (GBM) glomerulonephritis in rats. *Clin Exp Immunol* 109: 134-142, 1997.
6. **Kang JS, Wang XP, Miner JH, Morello R, Sado Y, Abrahamson DR, and Borza DB.** Loss of alpha3/alpha4(IV) collagen from the glomerular basement membrane induces a strain-dependent isoform switch to alpha5alpha6(IV) collagen associated with longer renal survival in Col4a3-/- Alport mice. *J Am Soc Nephrol* 17: 1962-1969, 2006.
7. **Kashtan CE.** Alport syndrome. An inherited disorder of renal, ocular, and cochlear basement membranes. *Medicine (Baltimore)* 78: 338-360, 1999.
8. **Katayama K, Kawano M, Naito I, Ishikawa H, Sado Y, Asakawa N, Murata T, Oosugi K, Kiyohara M, Ishikawa E, Ito M, and Nomura S.** Irradiation prolongs survival of Alport mice. *J Am Soc Nephrol* 19: 1692-1700, 2008.
9. **Katayama K, Kawano M, Naito I, Ishikawa H, Sado Y, Asakawa N, Murata T, Oosugi K, Kiyohara M, Ishikawa E, Ito M, and Nomura S.** Irradiation Prolongs Survival of Alport Mice. *J Am Soc Nephrol*, 2008.
10. **LeBleu V, Sugimoto, H., Miller, C.A., Gattone II, V.H. and Kalluri, R.** Lymphocytes are Dispensable for Glomerulonephritis but Required for Renal Interstitial Fibrosis in Matrix Defect Induced Alport Renal Disease. *Laboratory Investigation* in press: xx, 2008.
11. **Melo MD, Catchpole IR, Haggar G, and Stokes RW.** Utilization of CD11b knockout mice to characterize the role of complement receptor 3 (CR3, CD11b/CD18) in the growth of Mycobacterium tuberculosis in macrophages. *Cell Immunol* 205: 13-23, 2000.
12. **Mombaerts P, Iacomini J, Johnson RS, Herrup K, Tonegawa S, and Papaioannou VE.** RAG-1-deficient mice have no mature B and T lymphocytes. *Cell* 68: 869-877, 1992.

13. **Mundel P, Heid HW, Mundel TM, Kruger M, Reiser J, and Kriz W.** Synaptopodin: an actin-associated protein in telencephalic dendrites and renal podocytes. *J Cell Biol* 139: 193-204, 1997.
14. **Neilson EG.** The nephritogenic T lymphocyte response in interstitial nephritis. *Semin Nephrol* 13: 496-502, 1993.
15. **Ninichuk V, Gross O, Segerer S, Hoffmann R, Radomska E, Buchstaller A, Huss R, Akis N, Schlondorff D, and Anders HJ.** Multipotent mesenchymal stem cells reduce interstitial fibrosis but do not delay progression of chronic kidney disease in collagen4A3-deficient mice. *Kidney Int* 70: 121-129, 2006.
16. **Ophascharoensuk V, Pippin JW, Gordon KL, Shankland SJ, Couser WG, and Johnson RJ.** Role of intrinsic renal cells versus infiltrating cells in glomerular crescent formation. *Kidney Int* 54: 416-425, 1998.
17. **Prodromidi EI, Poulsom R, Jeffery R, Roufosse CA, Pollard PJ, Pusey CD, and Cook HT.** Bone Marrow Derived-Cells Contribute to Podocyte Regeneration and Amelioration of Renal Disease in a Mouse Model of Alport Syndrome. *Stem Cells*, 2006.
18. **Ries A, Engel J, Lustig A, and Kuhn K.** The function of the NC1 domains in type IV collagen. *J Biol Chem* 270: 23790-23794, 1995.
19. **Rodriguez-Iturbe B, Pons H, Herrera-Acosta J, and Johnson RJ.** Role of immunocompetent cells in nonimmune renal diseases. *Kidney Int* 59: 1626-1640, 2001.
20. **Soder S and Poschl E.** The NC1 domain of human collagen IV is necessary to initiate triple helix formation. *Biochem Biophys Res Commun* 325: 276-280, 2004.
21. **Strutz F and Neilson EG.** The role of lymphocytes in the progression of interstitial disease. *Kidney Int Suppl* 45: S106-110, 1994.
22. **Sugimoto H, Mundel TM, Sund M, Xie L, Cosgrove D, and Kalluri R.** Bone-marrow-derived stem cells repair basement membrane collagen defects and reverse genetic kidney disease. *Proc Natl Acad Sci U S A* 103: 7321-7326, 2006.
23. **Tipping PG and Holdsworth SR.** T cells in crescentic glomerulonephritis. *J Am Soc Nephrol* 17: 1253-1263, 2006.
24. **Tipping PG, Huang XR, Qi M, Van GY, and Tang WW.** Crescentic glomerulonephritis in CD4- and CD8-deficient mice. Requirement for CD4 but not CD8 cells. *Am J Pathol* 152: 1541-1548, 1998.

Supplementary Figure 1.

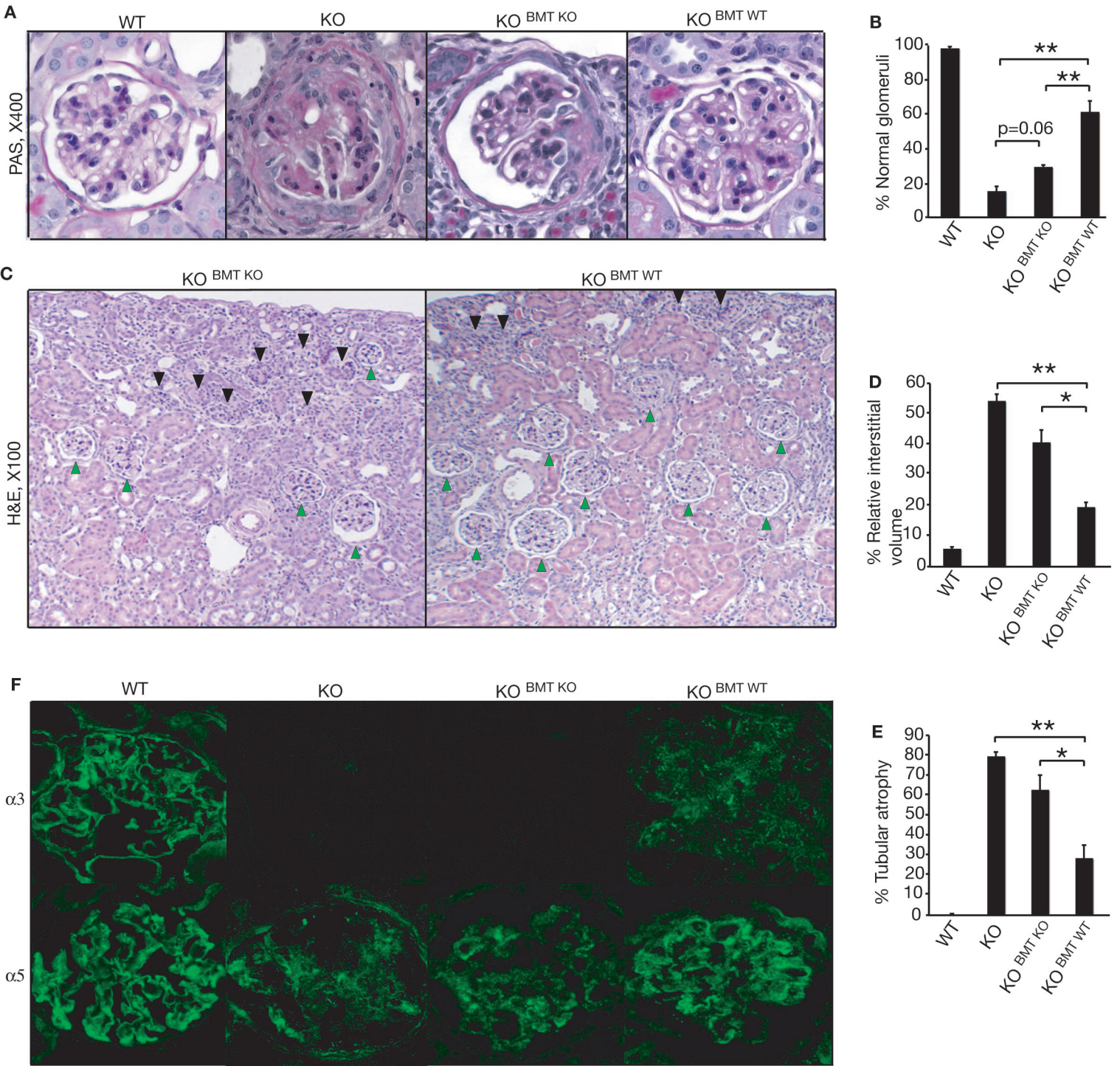

Supplementary Figure 2.

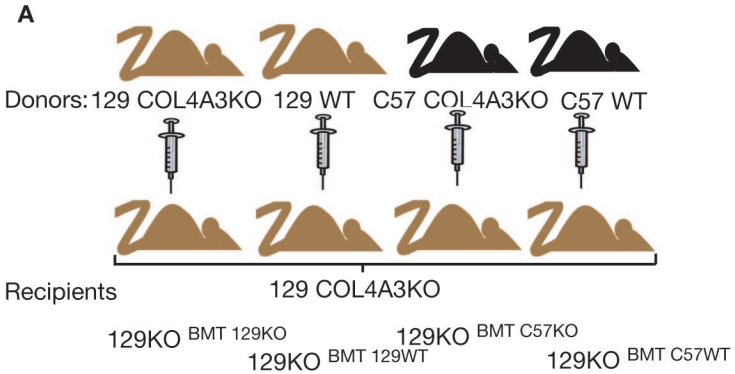

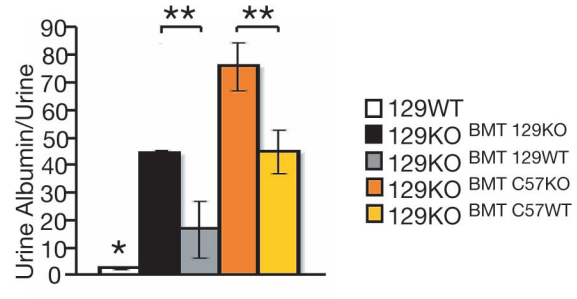

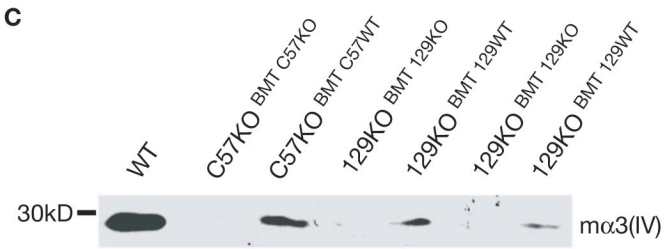

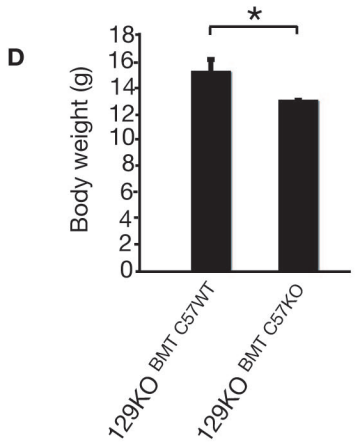

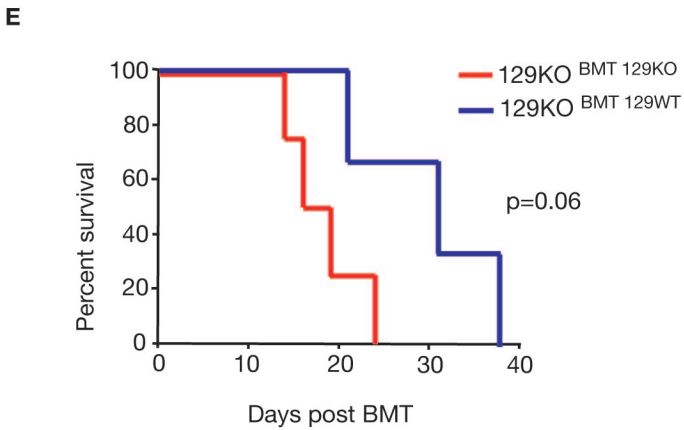

Supplementary Figure 3

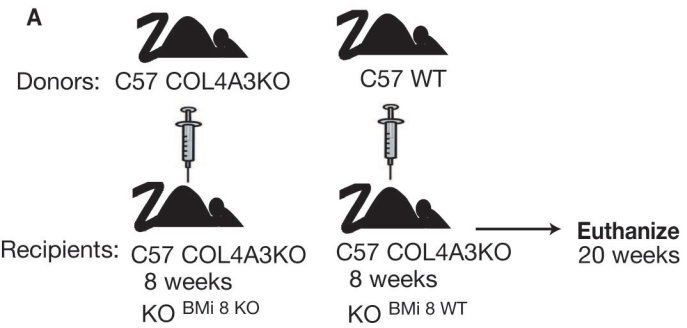

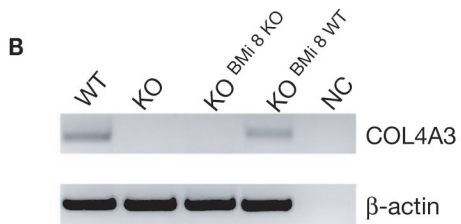

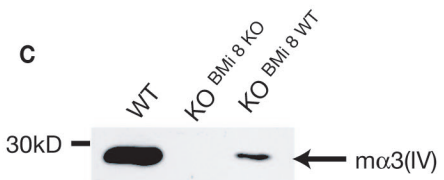

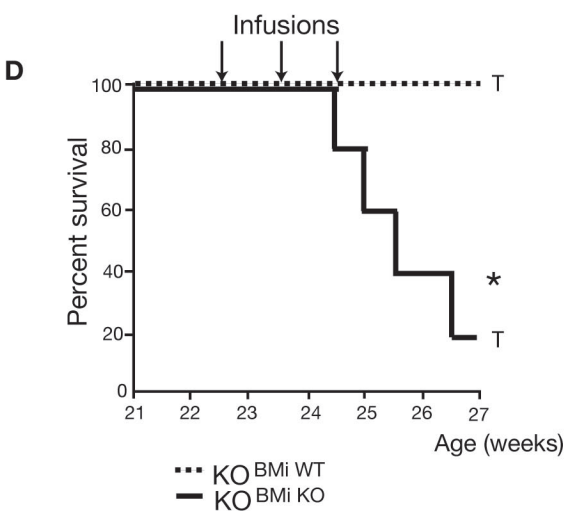

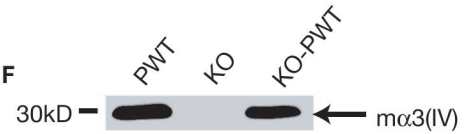

Supplementary Figure 4

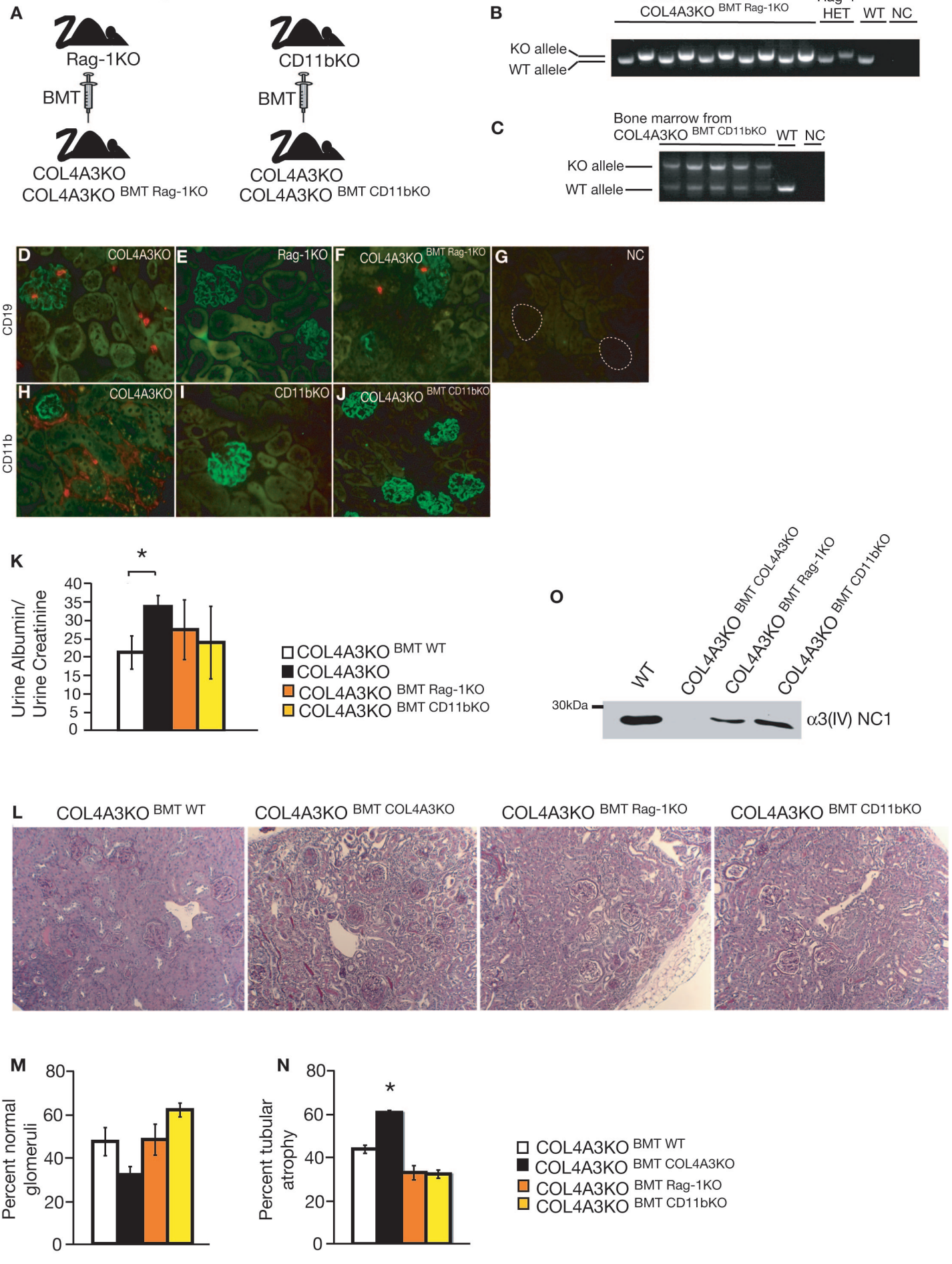

Supplementary Figure 5

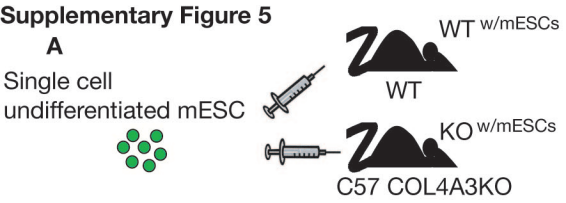

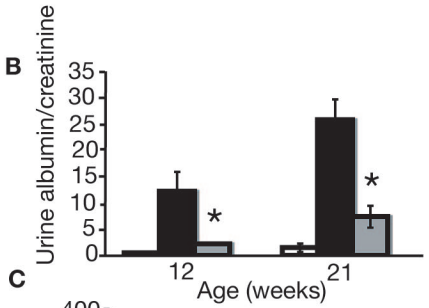

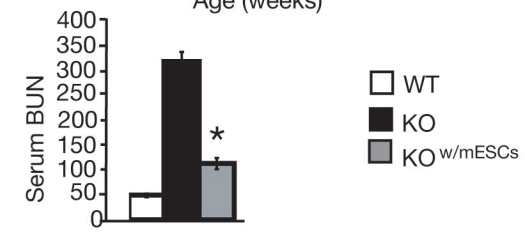

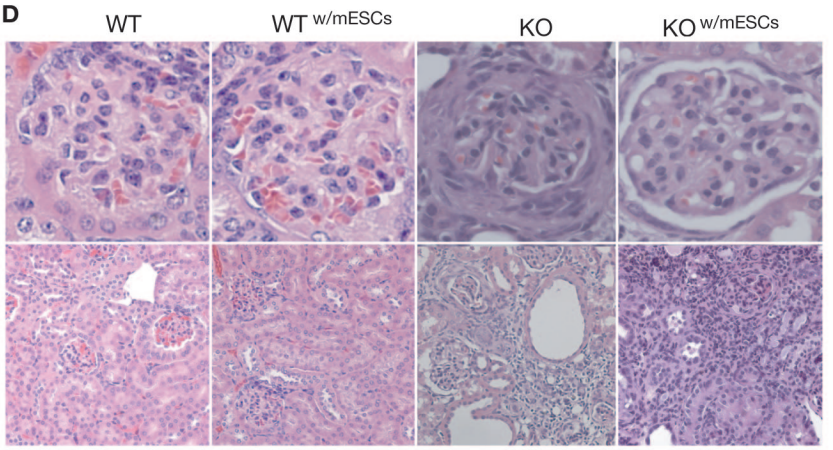

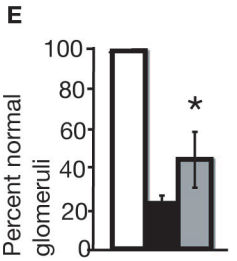

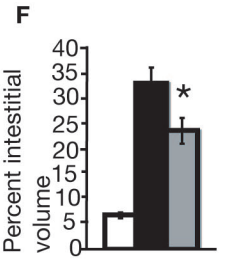

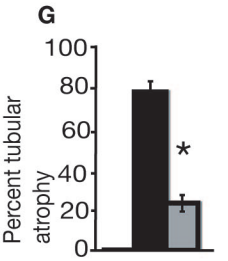

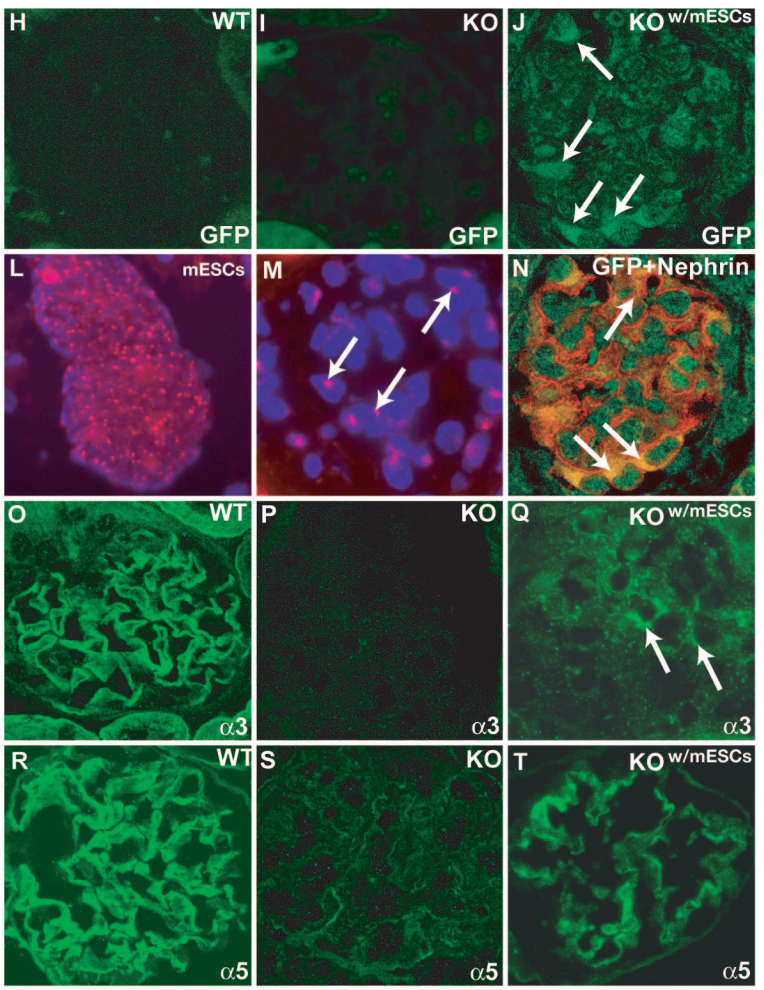

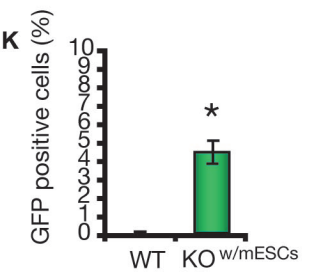

Supplementary Figure 6

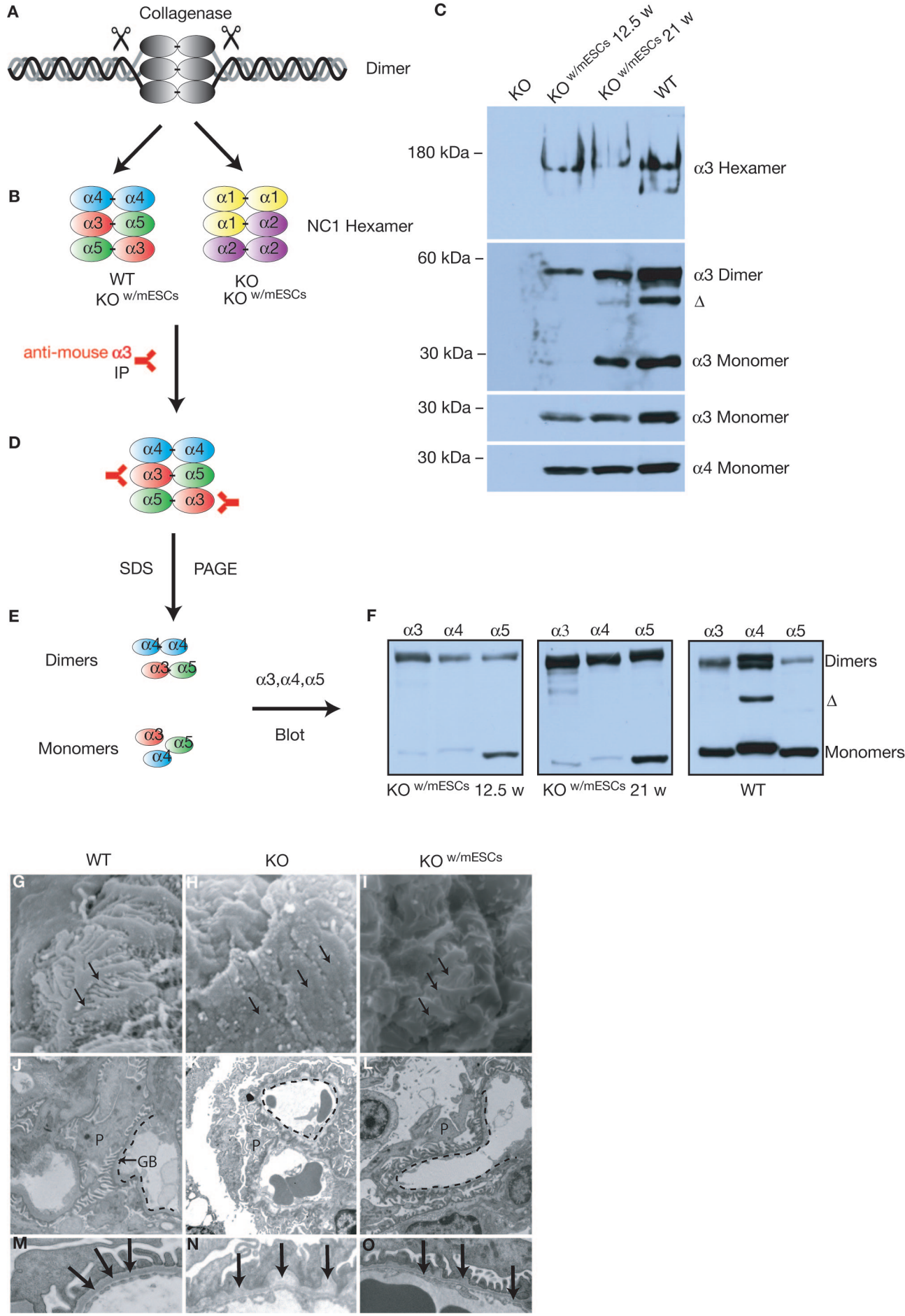

Supplementary Figure 7.

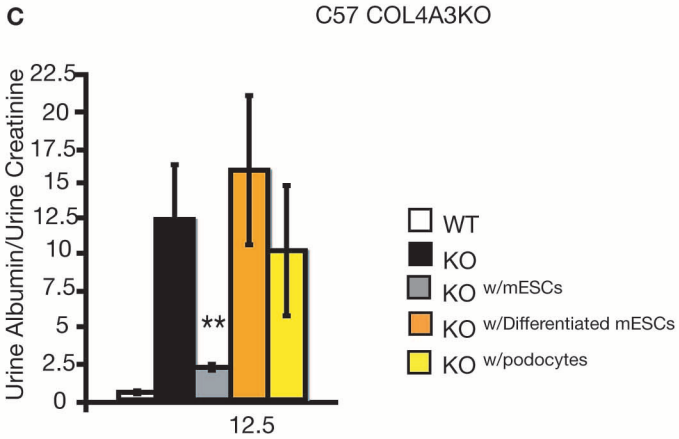

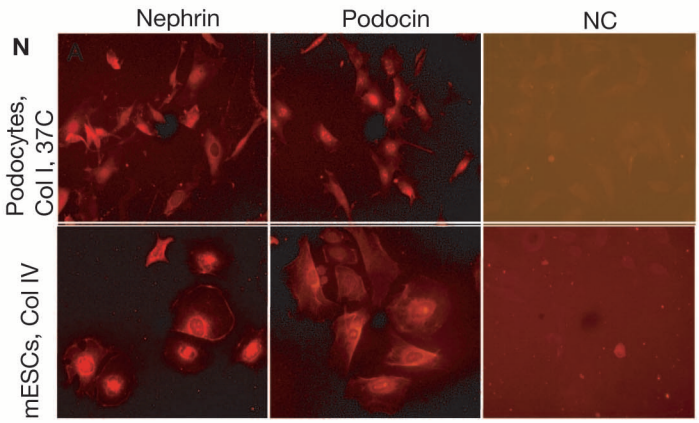

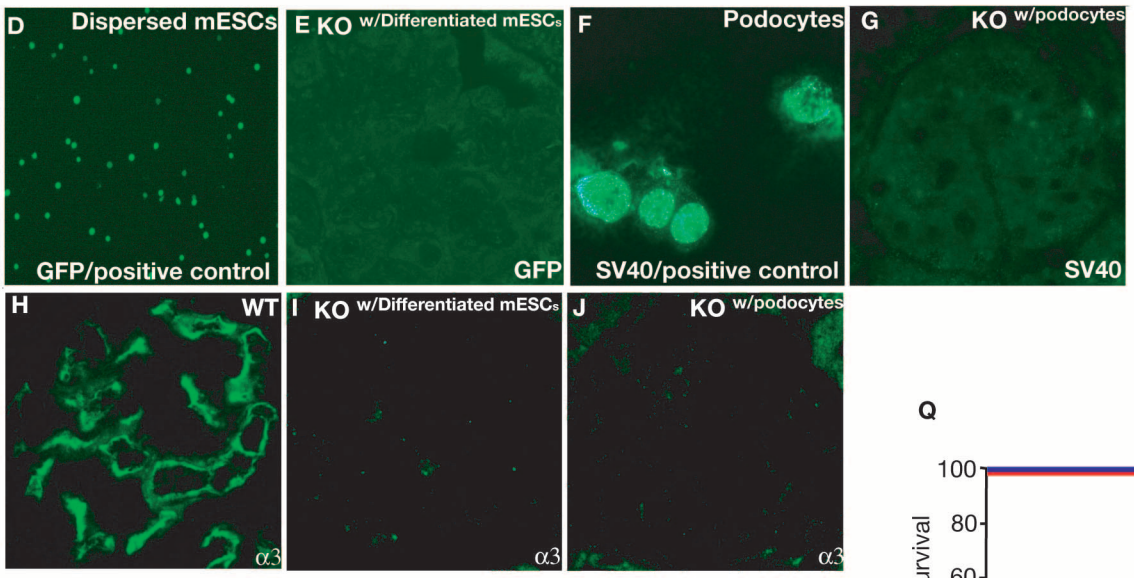

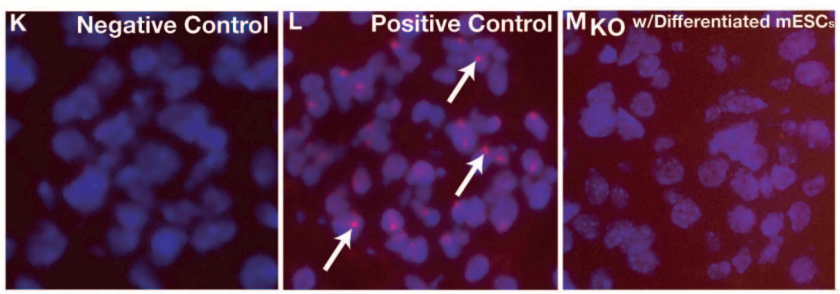

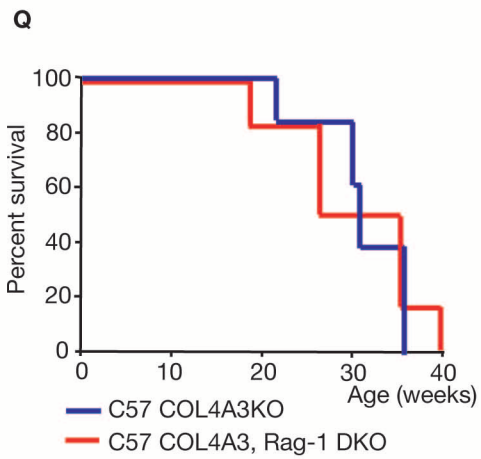

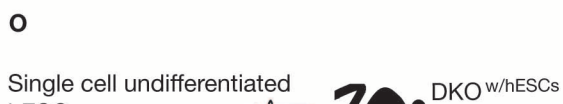

Supplementary Figure 8.

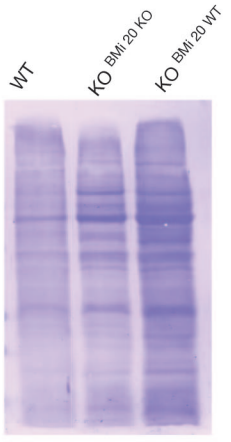

BMi (Figure 1)

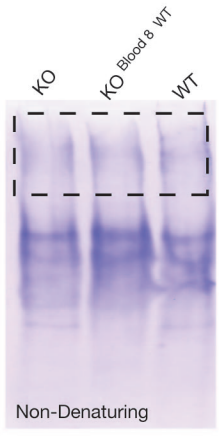

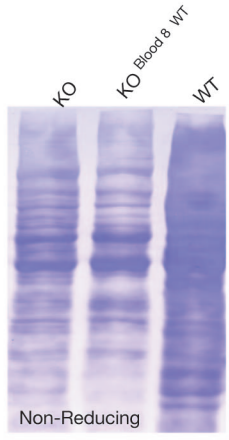

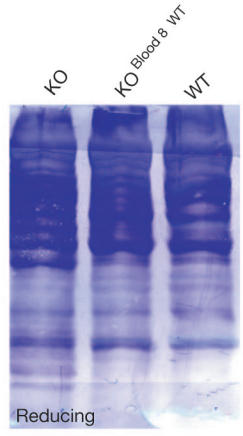

Blood transfusion (Figure 3)

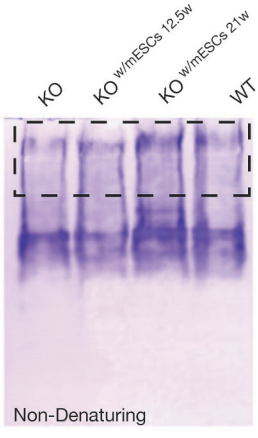

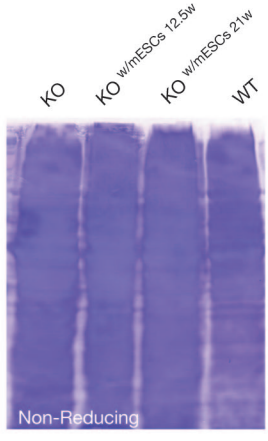

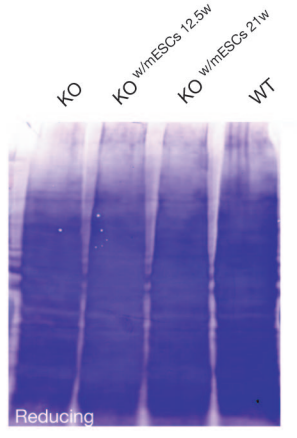

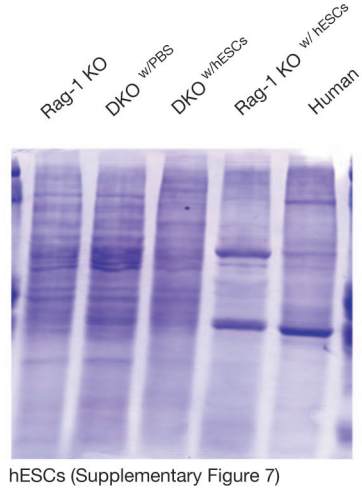

hESCs (Supplementary Figure 7)

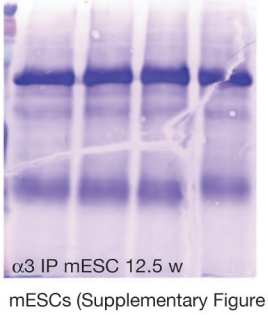

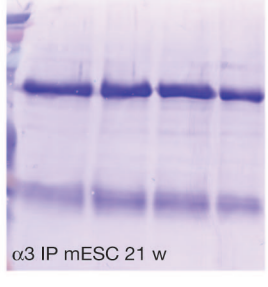

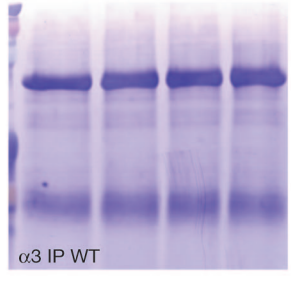

mESCs (Supplementary Figure 6)

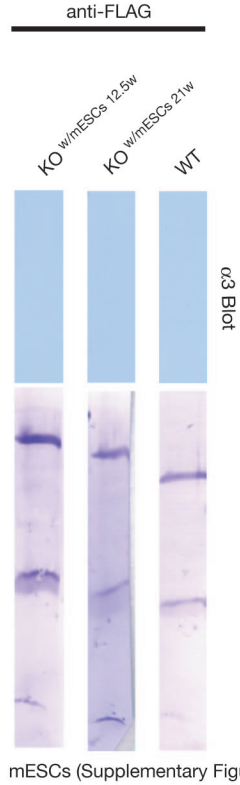

mESCs (Supplementary Figure 6)

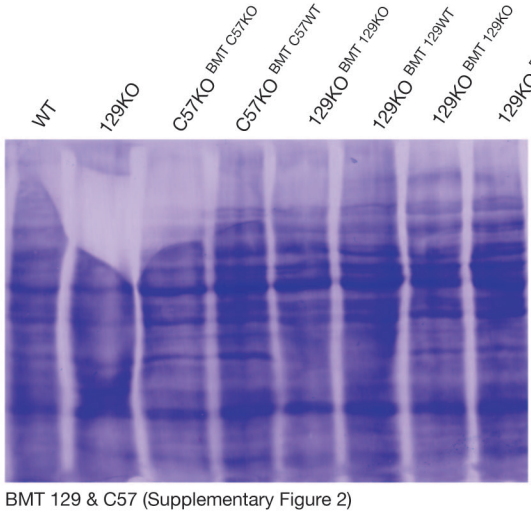

BMT 129 & C57 (Supplementary Figure 2)

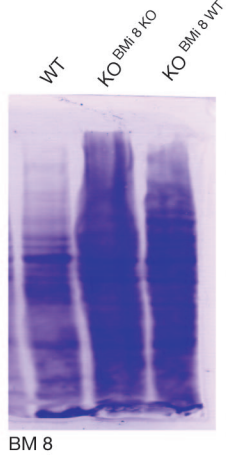

BM 8

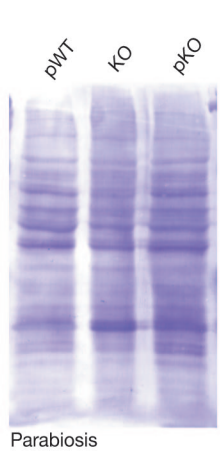

Parabiosis

(Supplementary Figure 3)